ELSEVIER

Journal of Alloys and Compounds 388 (2005) 153–157

Journal of ALLOYS AND COMPOUNDS

www.elsevier.com/locate/jallcom

Electrical and magnetic properties of $NdTiO_{3+\delta}$

E.J. Connolly[a,*], R.J.D. Tilley[b], A. Arulraj[c], R. Gundakaram[c], C.N.R. Rao[c]

[a] *Electronic Instrumentation Laboratory, TU Delft, Mekelweg 4, 2628 CD Delft, The Netherlands*
[b] *School of Engineering, University of Cardiff, PO Box 917, Cardiff CF2 1XH, UK*
[c] *Solid State and Structural Chemistry Unit, Indian Institute of Science, Bangalore 560012, India*

Received 30 June 2004; accepted 23 July 2004

Abstract

The electrical and magnetic properties of $NdTiO_{3+\delta}$ have been measured and correlated with unit cell parameters and composition of the samples. $NdTiO_{3+\delta}$ exhibited the $GdFeO_3$-type structure across the whole of the composition range, which in our investigations was found to extend approximately from $NdTiO_{3.05}$ to $NdTiO_{3.15}$. Over this range, the lattice contracted slightly, consistent with a rotation of the TiO_6 octahedra in the *a–c* plane. At compositions closest to $NdTiO_{3.05}$, the materials were semiconducting and displayed a ferromagnetic transition at a temperature of about 90 K. At compositions above about $NdTiO_{3.11}$, the materials were metallic and did not show any magnetic transitions. Several samples of composition close to $NdTiO_{3.11}$ showed a metal–insulator transition at typically ∼105 K. Electron microscopy revealed the presence of a microdomain texture in some samples, indicating that the results apply to an average structure rather than a genuine single phase. The results mirror those found for non-stoichiometric $LaTiO_{3+\delta}$ and can be explained in a similar fashion.

Keywords: Disordered systems; X-ray diffraction; Electronic transport; Magnetic measurements

1. Introduction

Oxides with the perovskite structure have long attracted attention because of the range of physical properties that they display and the ease with which these properties can be modified by chemical procedures. The parent structure consists of a cubic three-dimensional (3D) corner-linked array of BO_6 octahedra, with A cations occupying the 12-coordinate cage sites between them to give a composition of ABO_3. However, most ABO_3 phases show small distortions of the octahedra and off-centre displacements of the cations in the structure which have the effect of lowering the symmetry somewhat. One of the major structure types so produced is the $GdFeO_3$ type in which a certain amount of tilt of the octahedra has occurred [1] as shown in Fig. 1. $NdTiO_3$ belongs to this structure type and forms part of an important family of isostructural rare-earth titanates, $RTiO_3$, which have been extensively investigated structurally with a view to explaining their magnetic and electronic properties [2–5]. Measurements on the system $Nd_{1-x}A_xTiO_3$ (A = Ca, Sr, Ba) have revealed the existence of a compositionally dependent semiconductor to metal transition [6] and the magnetic properties of $Nd_{1-x}TiO_3$ have been shown to be similar to related $RTiO_3$ materials, especially $LaTiO_3$ [7–11]. The purpose of this paper is to extend these observations by presenting data on the variation of the electrical and magnetic properties of the phase $NdTiO_{3+\delta}$ ($Nd_yTi_yO_3$) as a function of the composition and microstructure of the samples.

2. Experimental

The starting materials were Nd_2O_3, ex Alfa industries (99.99%) and Johnson Matthey "Specpure" grade TiO_2 and Ti sponge. In all preparations, the Nd_2O_3 and TiO_2 powders were dried at 900 °C and weighed rapidly so as to minimise composition drift due to water absorption, especially by Nd_2O_3. Appropriate amounts of these chemicals were mixed in an agate mortar and then pressed in a die at a pressure

* Corresponding author. Tel.: +31 15 278 6518; fax: +31 15 278 6730.
E-mail address: e.j.connolly@its.tudelft.nl (E.J. Connolly).

0925-8388/$ – see front matter © 2004 Elsevier B.V. All rights reserved.
doi:10.1016/j.jallcom.2004.07.084

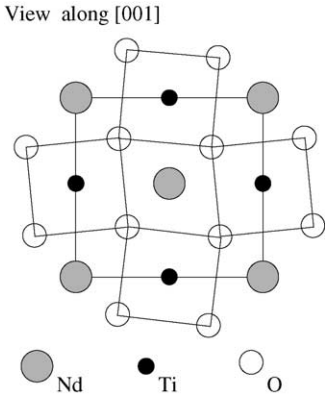

Fig. 1. A view of the $NdTiO_{3+\delta}$ structure along the [0 0 1] direction, showing the slightly rotated TiO_6 octahedra.

of 900 bar into 1-cm diameter pellets. The resultant pellets were arc-melted on a water-cooled copper hearth under flowing argon. After melting, some samples were annealed in sealed, evacuated silica tubes at 1000 °C for between 16 h and 5 days, and cooled slowly to room temperature. The global composition of most samples was determined gravimetrically by oxidation to $Nd_4Ti_4O_{14}$ in air at 1000 °C.

After reaction part of each sample was examined by powder X-ray diffraction using a Guinier–Hägg focusing camera (Expectron XDC-1000) employing strictly monochromatic Cu K_1 radiation and KCl as an internal standard ($a_0 = 6.2923$ Å at 25 °C). Lattice parameters were refined using standard least-squares techniques [12,13]. X-ray diffraction data for other samples were examined via a Siefert model XRD 3000TT diffractometer.

Selected samples were also examined by transmission electron microscopy. For this, small pieces of the arc-melted beads were crushed under *n*-butanol in an agate mortar. A drop of the resultant suspension was placed onto a copper grid that had previously been coated with a holey carbon film. Fragments of crystal were examined in a JEM 200CX transmission electron microscope fitted with a goniometer stage operating at 200 kV and equipped with a LaB_6 filament.

Electrical resistance of the samples was measured from 77 to 300 K using a standard four-probe method. For the purpose of these measurements, the arc-melted beads were ground on two parallel faces using standard wet/dry grinding/polishing techniques. Resistance measurements were performed using an evacuated Oxford Instruments type CF1104 cryostat, with an ITC-500 temperature controller. The sample temperature was held at the set-point temperature for about 30 min before taking any measurements, to ensure that thermal equilibrium had been established. A test current supplied by a Keithley type 224 constant current source was monitored via a Keithley type 181 nanovoltmeter. The temperature was monitored by means of an Au–0.3%Fe/chromel thermocouple. The whole process was automated and monitored by purpose-written software.

Magnetic susceptibility measurements in the range 18–300 K were carried out using a Lewis-coil force magnetometer.

3. Results

3.1. X-ray powder diffraction and composition

None of the starting materials were detected in any of the reacted beads by X-ray diffraction. However, the exact composition $NdTiO_{3.00}$ could not be prepared, and all our samples were slightly oxygen-rich. The X-ray powder patterns of the samples were in agreement with that published for single-crystal $NdTiO_3$ [14], but they were slightly variable from sample to sample. This was particularly noticeable in the sharpness of the lines and the degree of splitting of the (1 1 0) and (2 0 0) pair, and is not surprising in view of the non-equilibrium preparation method employed. Nevertheless, all the patterns could be indexed in terms of the expected orthorhombic unit cell. For an annealed sample of composition $NdTiO_{3.068}$, a unit-cell with $a = 0.5623 \pm 0.0002$ nm, $b = 0.7789 \pm 0.0001$ nm and $c = 0.5506 \pm 0.0001$ nm was found, in good agreement with the literature values of $a = 0.5589$ nm, $b = 0.7779$ nm, $c = 0.5495$ nm [14]. The composition range of the perovskite phase prepared in these experiments, determined from the X-ray powder photographs, was from approximately $NdTiO_{3.05}$ to $NdTiO_{3.15}$ − powder patterns from samples which were more oxygen-rich than this showed extra lines, which could be attributed to the layered phases related to $Nd_nTi_nO_{3n+2}$ system [15,16].

Details of the variation of lattice parameter with composition are given in Table 1 and Fig. 2. It was found that the *b*-axis varied less than both the *a*- and *c*-axes as the oxygen content increased. The *a*-axis seemed to decrease more rapidly than the *c*-axis, possibly indicating that the structure becomes more cubic as oxygen content is increased.

3.2. Transmission electron microscopy

The microstructure of the $NdTiO_{3+\delta}$ phase was variable. Sometimes crystal fragments showed a mottled contrast cor-

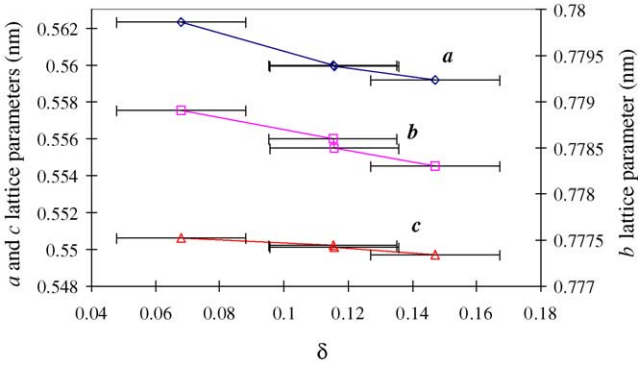

Fig. 2. Variation of the lattice parameters of $NdTiO_{3+\delta}$ as a function of δ error bars indicate the uncertainty in the value of δ.

Table 1
Lattice parameters[a] for $NdTiO_{3+\delta}$

δ[b]	a (Å)	b (Å)	c (Å)	Cell volume (Å^3)	R (Ω)	
					300 K	75 K
0.068	5.623 ± 0.0016	7.789 ± 0.0012	5.506 ± 0.0012	241.149	2.8	∼200
0.11A	5.599 ± 0.0015	7.785 ± 0.0016	5.501 ± 0.0016	239.778	4.5	∼250
0.11B	5.600 ± 0.0015	7.786 ± 0.0017	5.502 ± 0.0017	239.896	0.01	0.07
0.147	5.592 ± 0.0019	7.783 ± 0.0020	5.497 ± 0.0021	239.243	0.045	0.02
0.23	5.592 ± 0.0020	7.773 ± 0.0040	5.478 ± 0.0070	238.110	0.23	0.12

[a] Lattice parameter refinement using standard least-squares techniques [12,13].
[b] The value of δ shown (in $NdTiO_{3+\delta}$) is that obtained gravimetrically after oxidation to $Nd_4Ti_4O_{14}$ ($NdTiO_{3.5}$). The samples with $\delta = 0.11$A and $\delta = 0.11$B were insulating/semiconducting and metallic (with a M–I transition at $T \sim 105$ K), respectively (see Fig. 3).

responding to a microdomain texture, while other fragments showed no microdomains or other defects except those attributed to fracture damage. In a similar way, some electron diffraction patterns indicated that a supercell existed in which the a and c parameters were double that found by X-ray diffraction. These effects are very similar to those found in the $Nd_2Ti_2O_7$–$SrTiO_3$ system and illustrated earlier [15,16], so will not be shown here. In samples with an overall composition of above approximately $NdTiO_{3.2}$, electron microscopy showed that the perovskite phase co-existed with ordered layered perovskite phases of general formula $Nd_nTi_nO_{3n+2}$, as well as disordered structures very similar to those described previously.

3.3. Electrical conductivity

The preparation method utilised did not always give homogeneous samples, and sometimes different fragments of an arc-melted pellet showed slightly different conductivity. This was so even for samples annealed under vacuum for 5 days. The conductivity results did though, present a consistent pattern overall, with annealed samples showing improved consistency.

Samples which were closest in composition to $NdTiO_3$ behaved as insulators/semiconductors (i.e. increasing resistance with decreasing temperature). Typical resistance–temperature curves are shown in Fig. 3. The resistance of these (semiconducting/insulating) samples at 300 K was of the order of 1–10 Ω (see also Table 1), and this decreased smoothly as the oxygen content increased. At compositions greater than about $NdTiO_{3.11}$, metallic (i.e. decreasing resistance with decreasing temperature) behaviour was observed. Activation energies, E_a, estimated from the slope of ln(R) versus $1/T$ plots were ∼65 meV for both $\delta = 0.068$ and 0.11A samples. Metallic, or almost temperature-independent resistance properties were found in all samples in which the (3D) $NdTiO_{3+\delta}$ phases coexisted with layered perovskite (2D) phases,[1] provided that the (3D) perovskite phase was in the majority – see the $\delta = 0.23$ data shown in Fig. 3.

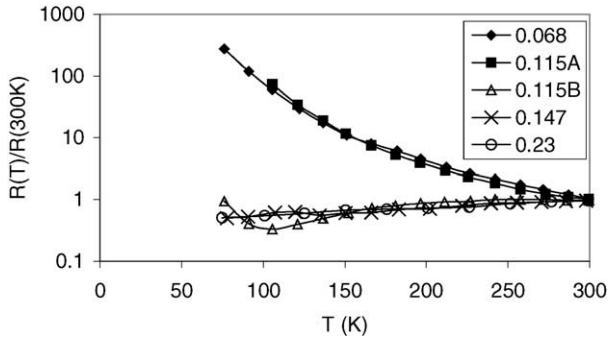

Fig. 3. Temperature variation of the relative resistance $R(T)/R(300\,K)$ for $NdTiO_{3+\delta}$, $\delta = 0.068$, 0.11A, 0.11B, 0.147, 0.23.

The resistance of the metallic samples at 300 K was generally between 0.01 and 0.1 Ω (see also Table 1). For several samples of composition close to $NdTiO_{3.1}$, a metal to insulator transition occurred at typically $T \sim 105$ K, similar to the $\delta = 0.11$B data shown in Fig. 3.

3.4. Magnetic susceptibility

The DC magnetic susceptibility data for three samples are shown in Fig. 4. Also shown in the inset of Fig. 4 are plots of reciprocal susceptibility versus temperature. The samples $NdTiO_{3+\delta}$ with $\delta = 0.07$ (insulating) and $\delta = 0.11$ (metallic) show ferromagnetic transitions as can be seen in the reciprocal susceptibility data, while the sample with $\delta = 0.23$ (also metallic) does not. The transition temperatures T_{FM}, for the $\delta = 0.07$ and 0.11 samples, are approximately 90 and 60 K, respectively. Plots of susceptibility with field, shown in Fig. 5, confirm the occurrence of ferromagnetism below T_{FM}. The sample with $\delta = 0.07$ shows field-dependent magnetic susceptibility at temperatures below the magnetic ordering temperature, both while increasing and decreasing the field (for clarity only the increasing field data is shown, but the decreasing field data was almost identical). In contrast, the sample with $\delta = 0.23$ does not show any significant field dependence (see inset of Fig. 5). For the samples $\delta = 0.07$ and 0.11, a Curie–Weiss fit of the reciprocal magnetic susceptibility data well above T_{FM} gave Weiss temperatures of ∼−25 K, indicating a high-temperature antiferromagnetic order.

[1] The layered (2D) materials $Nd_nTi_nO_{3n+2}$ are electrically insulating [17].

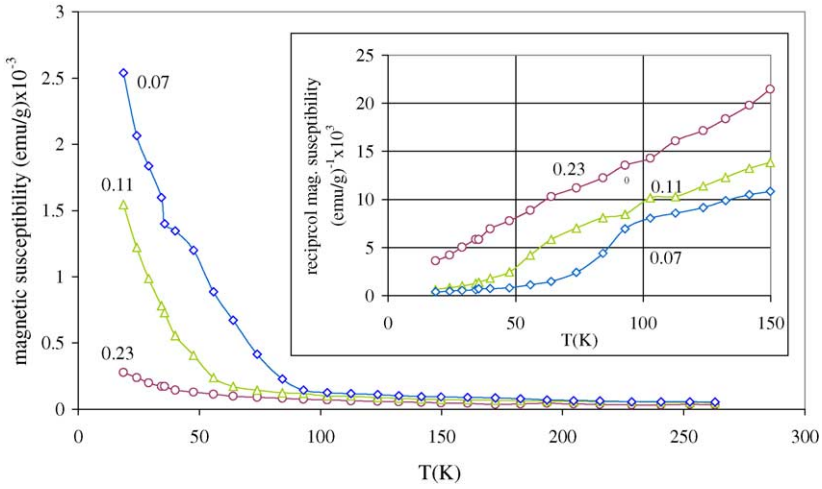

Fig. 4. Temperature variation of the magnetic susceptibility and inset, reciprocal magnetic susceptibility, of $NdTiO_{3+\delta}$ with $\delta = 0.07$ ($T_{FM} \sim 90$ K; insulator/semiconductor), $\delta = 0.11$ ($T_{FM} \sim 60$ K; metallic), and $\delta = 0.23$ (no magnetic transition observed down to 18 K; metallic).

4. Discussion

The present study shows that the $NdTiO_{3+\delta}$ phase was oxygen-rich in our preparations. Moreover, the samples were never completely homogeneous. Nevertheless, the results obtained are internally consistent and allow one to arrive at reasonable conclusions about the material. In general, we estimated a (single phase, 3D perovskite) composition range from (probably below) $\delta \sim 0.05$ to ~ 0.15 for our specimens. It is likely, in common with other non-stoichiometric oxides that this composition range is temperature-sensitive. Careful equilibration experiments are needed to map it fully.

It is unlikely that the material contains an excess of oxygen over the composition $NdTiO_{3.0}$, and the true composition is probably better represented by $Nd_yTi_zO_{3.0}$, that is to say, there is a population of vacancies on either the A (Nd) sites or the B (Ti) sites or on both. In terms of an ionic model, the charges on both the Nd (3+) and O (2−) are fixed but the Ti can adopt a nominal charge of either 3+ or 4+. Because in our preparations the Nd:Ti ratio was maintained at 1:1, and because oxidation did not show any other phases apart from $Nd_4Ti_4O_{14}$, it is likely that this ratio still holds in the perovskite phase. In such a case, the composition of a given sample would involve vacancies on both the Nd and Ti sites, leading to a formula $Nd_yTi_yO_{3.0}$ which includes a small population of Ti^{4+} ions present to maintain charge balance.

The fact that the unit cell decreases (see Table 1) as the composition becomes oxygen-rich supports a vacancy hypothesis. Additionally, substitution of Ti^{3+} ($r_{ionic} \sim 0.81$ Å) by Ti^{4+} ($r_{ionic} \sim 0.745$ Å) contributes to the lattice contraction. It is seen that the *b*-axis hardly changes, which means that the actual dimension of the octahedra (or at least the octahedral diagonal) alters very little. The changes observed are then consistent with a rotation of the octahedra in the *a*–*c* plane towards a more cubic orientation, coupled with a slight contraction due to the vacancy population plus the partial substitution of smaller Ti^{4+} for Ti^{3+}. In our samples, this process was stable up to a composition of about $NdTiO_{3.15}$, that

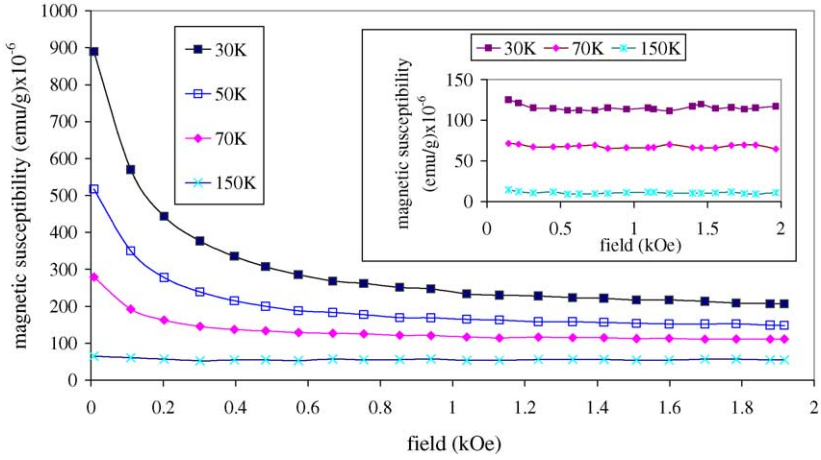

Fig. 5. Field variation of magnetic susceptibility (increasing field) for $NdTiO_{3.07}$ and inset for $NdTiO_{3.23}$.

is to say about $Nd_{0.95}Ti_{0.95}O_{3.00}$, after which layered phases of the $Nd_nTi_nO_{3n+2}$ system [16] started to appear.

The domain contrast observed via transmission electron microscopy [15,16] may also be associated with this vacancy population. Similar contrast has been reported for $LaTiO_3$ [9], $Nd_2Ti_2O_7$–$SrTiO_3$ [15,16] and $La_{0.5}Li_{0.5}TiO_3$ [18]. This type of contrast can be explained by assuming that the microdomains are composed of ordered A ion vacancies, but similar contrast would also result from the unit cell variation found, irrespective of the cause of the change. At present we do not have sufficient evidence to discriminate between these two models. Further studies to clarify the position are underway and will be reported in the future.

The physical properties found by us are similar to that recorded for $LaTiO_3$ [8–11], in which an initial semiconducting (and ferromagnetic) regime also gives way to a metallic (and paramagnetic) region. The composition of the transition to the metallic state in our samples, approximately $NdTiO_{3.11}$, is a more oxygen-rich composition than that found for $LaTiO_{3+\delta}$ (metallic for $\delta > \sim 0.02$). As the increase of oxygen content is associated with a decrease in the lattice parameters of the cell, it seems that either the smaller Nd ion needs a greater cell contraction (compared to the larger La ion) before the transformation of the semiconducting behaviour to metallic, or a reduction in disorder caused by rotation of the octahedra in the *a*–*c* plane with increasing δ (i.e. Anderson-type transition), or a mixture of both these effects enable the semiconductor–metallic transition. Otherwise, the two systems seem to be quite analogous in their properties.

The magnetic transitions are ascribed to the onset of ferromagnetism, as in the case of $LaTiO_{3+\delta}$ [8,9]. These disappear at a composition close to when the material takes on the metallic character just described. The susceptibility measurements on these samples suggest that the ferromagnetic nature of $NdTiO_{3.07}$ and $NdTiO_{3.11}$ is most likely to be due to spin-canting.

Acknowledgements

E.J.C. is indebted to the School of Engineering, University of Cardiff, for a grant that made this study possible. The authors also thank J. Sloan for assistance with the electron microscope study.

References

[1] H.D. Megaw, Crystal Structures, Saunders, Philadelphia, PA, 1973, p. 298.
[2] D.A. McLean, H.N. Ng, J.E. Greedan, J. Solid State Chem. 30 (1979) 35.
[3] J.E. Greedan, J. Less Common Met. 111 (1985) 335.
[4] P. Ganguly, O. Parkash, C.N.R. Rao, Phys. Stat. Sol. A 36 (1981) 669.
[5] D.A. McClean, K. Seto, J.E. Greedan, J. Solid State Chem. 40 (1981) 241.
[6] C. Eylam, H.L. Ju, B.W. Eichhorn, R.L. Greene, J. Solid State Chem. 114 (1995) 164.
[7] G. Amow, J.E. Greedan, J. Solid State Chem. 121 (1996) 443.
[8] M.J. MacEachern, H. Dabkowska, J.D. Garrett, G. Amow, W. Gong, G. Liou, J.E. Greedan, Chem. Mater. 6 (1994) 2092.
[9] F. Lichtenberg, D. Widmer, J.G. Bednorz, T.B. Williams, A. Reller, Z. Phys. 82 (1991) B211.
[10] Y. Okada, T. Arima, Y. Tokura, C. Murayama, N. Mori, Phys Rev. B 48 (1993) 9677.
[11] D.A. Crandles, T. Timusk, J.E. Greedan, Phys. Rev. B 44 (1991) 13250.
[12] P.E. Werner, Arkiv Kemi. 31 (1969) 513.
[13] P.A. Stadelmann, Ultramicroscopy 21 (1987) 131.
[14] JCPDF-ICDD entry 33-942, Nat. Bureau Stand. (U.S.), Monogr. 25 (1981) 18.
[15] J. Sloan, R.J.D. Tilley, J. Solid State Chem. 121 (1996) 324.
[16] E. Connolly, J. Sloan, R.J.D. Tilley, Eur. J. Solid State Inorg. Chem. 33 (1996) 371.
[17] E. Connolly, Ph.D. Thesis, University of Wales, Cardiff, 1996.
[18] A. Varez, F. Garcia-Alvaro, E. Moran, M.A. Alario-Franco, J. Solid State Chem. 118 (1995) 78.